A Probabilistic Model for Correcting the Directional Sensitivity of Optical Probe Measurements

Boung Wook Lee and Milorad P. Dudukovic
Chemical Reaction Engineering Laboratory (CREL), Energy, Environmental, and Chemical Engineering Dept., Washington University in St. Louis, St. Louis, MO 63130

DOI 10.1002/aic.14860
Published online May 27, 2015 in Wiley Online Library (wileyonlinelibrary.com)

A probabilistic model is introduced for correcting the directional sensitivity of the optical probe technique routinely used to determine gas holdup and bubble dynamics in gas-liquid systems. Measurements from optical probes oriented at various angles were collected from the tapered end of optical probes in regions where approximately unidirectional and bubbly flow conditions were observed. Based on logical assumptions, constitutive equations for a probabilistic model were formulated, and contributions to the overall local gas phase holdup from bubbles traveling in two opposite directions were quantified. The results demonstrate a novel and useful way to interpret optical probe measurements. © 2015 American Institute of Chemical Engineers *AIChE J*, 61: 3516–3527, 2015
Keywords: optical probe, directional sensitivity, probabilistic model, gas liquid flow

Introduction

Assessing gas phase dispersions in two or three phase systems remains a challenge in multiphase reaction engineering, mainly due to the lack of fundamental understanding of the gas phase flow field and the complex intraphase and interphase interactions associated with it.[1–3] The majority of the experimental and computational research directed at quantifying gas phase dispersions, intraphase and interphase mixing, and gas-liquid transport has thus far relied on the concept of phase holdup,[4,5] that is, the local and/or global volume fraction occupied by a particular phase. Numerous experimental techniques for measuring phase holdups have been developed,[6–8] and their results used to validate phenomenological and computational models at various scales.[9–19]

Despite all the recent advances, phase dispersion properties obtained from multiphase computational fluid dynamics models still require precise validation via means of reliable experimental techniques.[20,21] For large-scale vessels, even the most detailed models possess significant limitations due to unverified simplifying assumptions, correlations, or extrapolations, and/or they require too much computational power. Further development and utilization of reliable and affordable visualization techniques are therefore invaluable for assessing of industrial multiphase reactors.[22]

In our Chemical Reaction Engineering Laboratory (CREL) and elsewhere,[23–27] the optical probe technique has been proven to be one of the most versatile tools for characterizing gas phase dispersions by measuring local gas phase holdups and bubble dynamics. Two types of microsized probes are available: optical and conductivity. Optical probes offer several distinct advantages: simple setup, easy signal interpretation, a high signal-to-noise ratio, a wide range of media in which they can be used and many operating conditions including high temperature and pressure.[28,29] First adopted in CREL by Xue,[29] the optical probe technique has been successfully applied to bubble columns,[20,30] slurry bubble columns,[31] gas-liquid stirred tanks,[21,32,33] and pressurized autoclaves.[21,34,35] Tapered end probes in particular have proven useful for wide range of applications.

Despite all the advantages, a significant and often-neglected disadvantage of the tapered end optical probe technique[21,29] remains: potential bias when the tip is employed in "improper" orientations. The technique is invasive by nature and the bubbles must pierce the probe tip in order to be detected; as a consequence, the probe can detect only bubble populations traveling in certain directions. Chances for the probe to miss a significant number of bubbles always exist, especially if the probe tip is much larger than the bubbles and/or the tip is not facing the main flow direction. While several studies have provided general guidelines on how big the probe tip must be, for example, Mueller,[21] no theoretical foundation has been firmly established for correcting the directional sensitivity of the technique. Notable works which touch on the potential error due to directional sensitivity and attempt to correct it include those by Enrique Juliá et al.,[28] Mueller and Dudukovic,[36] Lee and Dudukovic,[32] and Groen.[37] In all of these works, with the exception of the work by Groen,[37] the authors reported "true" (unbiased) local gas holdups based on the measurement results obtained from tips that were oriented to face the main flow directions, where either the largest local gas holdups were measured or practically all of the bubbles were assumed to have been captured by the probe. Groen[37] suggested a simple model to correct for the directional sensitivity, but it has not been adapted by other researchers most likely due to what he termed "a crude assumption" involved.

Correspondence concerning this article should be addressed to B. W. Lee at boungwooklee@go.wustl.edu.

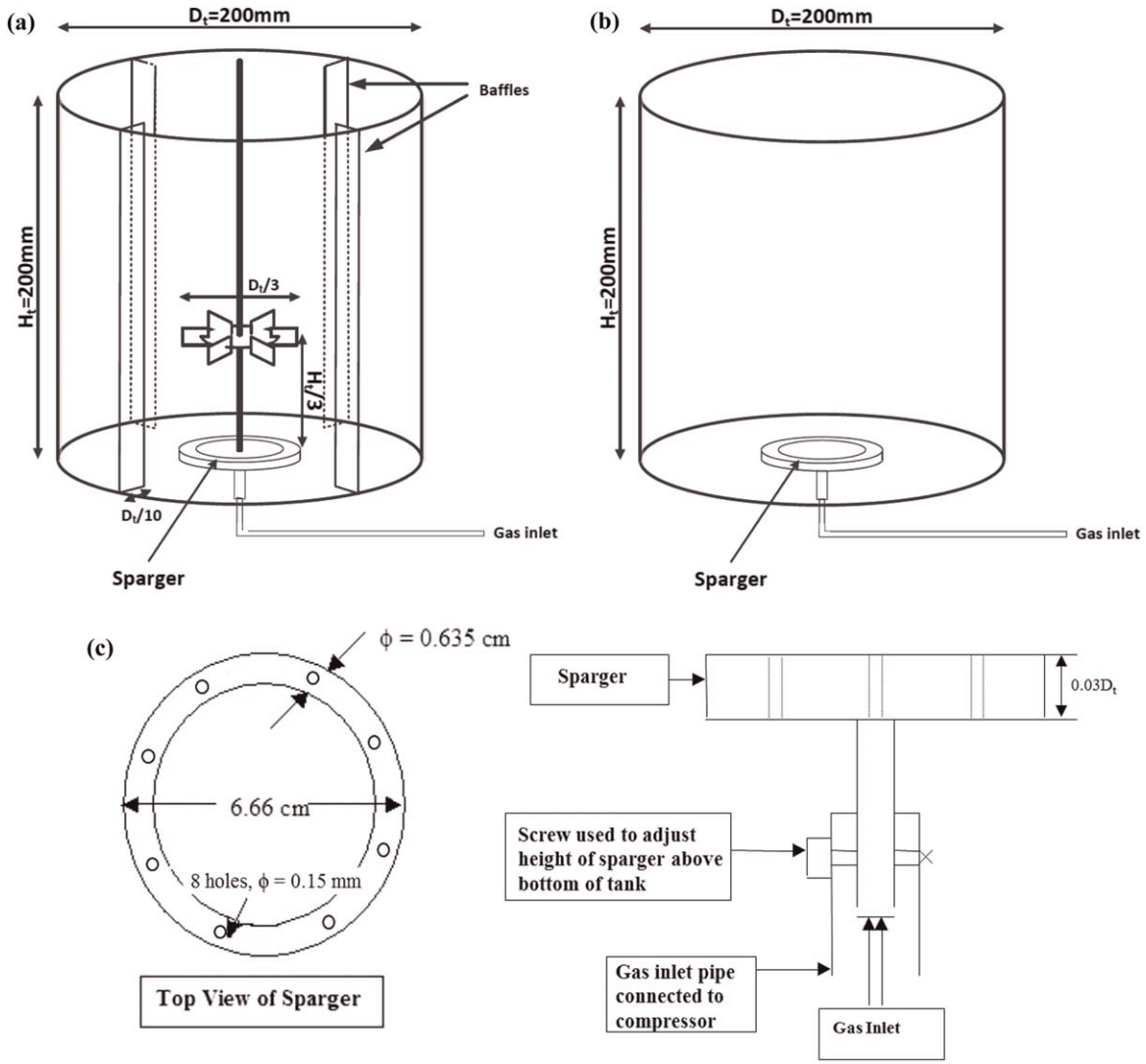

Figure 1. (a) Stirred tank (equipped with a Rushton Turbine (RT) and the baffles), (b) sparged tank, and (c) ring sparger (figure modified From Rammohan, Characterization of Single and Multiphase Flows in Stirred Tank Reactors, 2002, © Department of Chemical Engineering, Washington University in St. Louis, reproduced with permission).

While using the optical probe technique in strictly unidirectional flow may result in "true" and unbiased representation of gas holdup, in other flow conditions, for example, bubbly flows where bubbles fluctuate and move in various directions, it is questionable whether the optical probe measurements yield "true" gas holdup. A comprehensive method or model capable of correcting for directional sensitivity is needed.

Experimental Setup and the Optical Probe

Gas-liquid stirred tank

The gas-liquid stirred tank reported in our previous studies[32,33] was used to approximate three flow conditions: one unidirectional flow and two bubbly flow conditions. To mimic the unidirectional flow, the stirred tank was equipped with a standard Rushton Turbine (RT) and four baffles on the tank wall. For bubbly flow conditions, two experimental setups were used: the stirred tank equipped with a RT and the baffles, and bare tank with the gas sparger, that is, the sparged tank. Filtered air and tap water were used for the gas phase and the liquid phase. Figure 1 shows the schematics of the two setups and the sparger.[38]

Approximately unidirectional flow

Flooding, loading, and fully recirculated regimes (Figure 2) were identified in the stirred tank.[36,39,40] The three regimes are marked by distinct differences in the regions which the bubbles occupy and the predominant local bubble movement direction. In the flooding regime, bubbles from the sparger are not effectively dispersed throughout the tank and a bubble column-like behavior (bubbly flow) is observed in the central region. In the outer regions, very few to no bubbles are observed. In the loading regime, bubbles from the sparger are dispersed just enough to occupy the upper part of the tank (above the impeller discharge plane) in both the inner and outer regions, and bubbles show a near-unidirectional movement toward the top of the tank (free surface). In the fully recirculated regime, bubbles occupy all regions of the tank and recirculation loops are observed below and above the impeller discharge plane. As the turbine

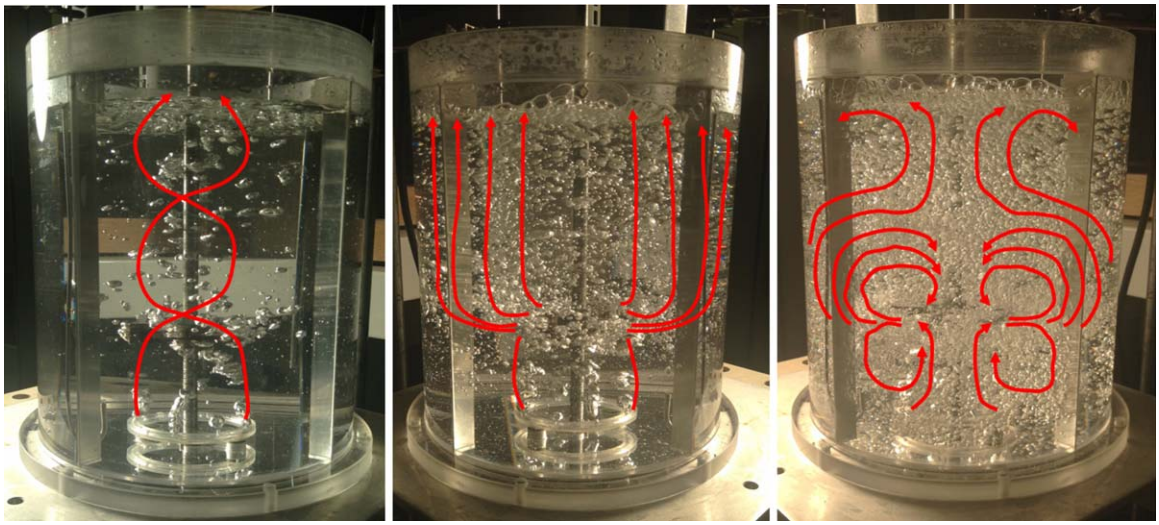

Figure 2. The three flow regimes of a gas-liquid stirred tank.

[Left, the flooding regime; middle, the loading regime; right, the fully recirculated regime. Red lines with arrows represent predominant local bubble movement directions.] [Color figure can be viewed in the online issue, which is available at wileyonlinelibrary.com.]

RPM is increased and the flow becomes more dispersed, smaller recirculation loops are observed in regions close to the free surface, tank walls, and the baffles.

Careful visual inspection of the three flow regimes at various operating conditions and regions revealed the most distinct unidirectional flow region to be the upper outer region of the loading regime. Accordingly, our optical probe was employed at an axial height of $h = 11.5H$ (H = liquid height), a radial position $r = 0.9R$ (R = radius of the stirred tank), and 45° from the baffle (midway between the two baffles), under operating conditions of 515 RPM and 0.408 m^3/min of gas flow at standard temperature and pressure. These conditions correspond to operating dimensionless parameters of $Fl = 0.045$ and $Fr = 0.5$. Fl and Fr represent the Flow Number and the Froude Number, respectively, and are the two mostly commonly used dimensionless operating parameters for assessing the flow regime and quantifying the overall degree of dispersion of an air-water stirred tank.[32,36,39,40]

Bubbly flow

For bubbly flow conditions, optical probes were employed in both experimental setups (stirred tank and sparged tank) to investigate whether the degree of gas phase dispersions had significant effects on our model results. For the stirred tank, our optical probe was deployed in the region, where only a small number of bubbles was observed, at an axial height of $h = 13.5H$ (H = liquid height), a radial position $r = 0.4R$ (R = radius of the stirred tank), and 45° from the baffle (midway between the two baffles) under the operating condition of 230 RPM and 0.184 m^3/min ($Fl = 0.045$ and $Fr = 0.1$). For the sparged tank, our optical probe was deployed in a region where a relatively large number of bubbles was observed, at an axial height of $h = 13.5H$ (H = liquid height) and in the center of the tank under operating condition of 0.524 m^3/min.

Optical probe and data acquisition

For our probes, we chose 105/125/250 μm core/cladding/coating diameter multimode optical fibers from Thorlabs. The fibers were first tapered and polished via methods outlined by Mueller[21] to have their tips be of conical shape. The finished fibers were then epoxied into 1/8 in.-diameter stainless steel tubes and inserted into the tank from the top (free surface). For all three operating conditions investigated, measurements were collected at impact angles (θ) ranging from 0° (facing the main flow direction, toward the bottom of the stirred tank and sparged tank) to 330° (Figure 3). For each run, the voltage signal from the photodiodes (Thorlabs PDA36A) was collected at a rate of 40 kHz (PowerDAQ PD-BNC-16) for 1500 data acquisition frames, a total

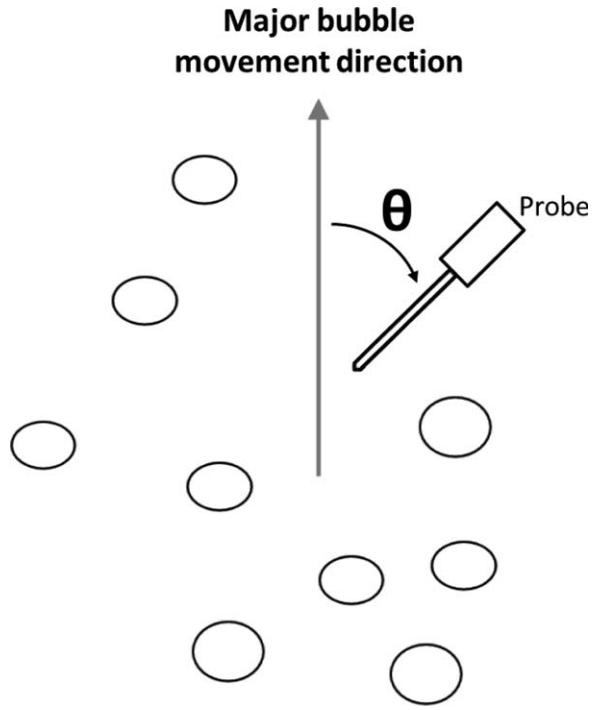

Figure 3. "Needle-like" probe in gas-liquid system.

[Circles represent gas bubbles and θ represents the impact angle (angle away from the main flow direction and major bubble movement) at which the probe is employed.]

duration of 691.2 s. For the two setups we investigated, the majority of the bubbles are at least by an order of magnitude larger ($\geq$1.05 mm) than the optical probe tip as reported by our group's previous work[21,29]; hence the measurement inaccuracy caused by drifting and/or deformation of bubble interfaces for "small" bubbles can be ignored.[41]

Data Processing

The collected signals were normalized, first by subtracting the minimum voltage observed during the whole measurement time, and then dividing this value by the difference between a reference voltage and the minimum voltage observed. The reference voltage was set to a value that constrained the dry tip normalized voltage between 0.8 and 1.2. In equation form, this is equivalent to

$$V_{\text{norm}} = \frac{\text{Meausred voltage} - \text{Minimum voltage}}{\text{Reference voltage} - \text{Minimum voltage}} \quad (1)$$

After checking for bimodality of the signals, the normalized signals were converted into binary signals; gas holdups and bubble counts were obtained via the procedure detailed in our previous works.[32,33]

Directional Sensitivity of "Needle-Like" Probes

There are numerous literature reports based on "needle-like" probe techniques (which include our optical probe technique), as summarized by Boyer et al.,[6] yet only a few consider the directional dependency of their results. To the author's knowledge, the most detailed discussion is provided by Bombač et al.,[39] who included the directional sensitivity of their measurements inside a reactor region where unidirectional flow is observed. For their microresistivity probe, which operates on a similar principle as our optical probe and also has a tapered tip, the magnitude of directional dependency was found to be insignificant up to the an impact angle (θ) of 90°, suggesting the acceptance angle (β) of their probe to be 180°. As the impact angle (θ) increased to 120°, only a slight reduction (10%) in the measured holdup values was reported, and measurement results beyond $\theta = 150°$ were not provided.

From our group, Mueller and Dudukovic[36] and Lee and Dudukovic[32] noted the optical probe's directional sensitivity, but no discussion regarding the magnitude of directional dependency was included. In theory, the two techniques (conductivity and optical probes) should have equivalent directional sensitivities. However, as there exist numerous attributes which may cause differences, for example, the exact tip shape (angle) and size, processing algorithms, detector sensitivities, bubble size distribution, velocity, and shape, here we present our optical probe's directional sensitivities for the three flow conditions we investigated.

Approximate unidirectional flow

Figure 4 shows the gas holdups and bubble counts obtained at impact angles ranging from $\theta = 0°$ (Figure 3) to 330° at intervals of 30° for the approximate unidirectional flow condition. The results are very similar to what was previously reported by Bombač et al.[39] with their conductivity probe. As the impact angle (θ) increased from 0° to 90°, that is, up to acceptance angle (β) of 180°, the gas holdups and bubble counts remained relatively constant; as the impact angle (θ) increased from 90° to 180°, the two parameters decreased and reached their minimum values before increasing once again as θ increased. The minimum gas holdup and the minimum bubble count observed at $\theta = 180°$ were approximately 45 and 60% of what was observed when the probe was oriented to face the main flow direction ($\theta = 0°$), respectively.

The fact that a significant number of bubbles were detected and contributed to the local gas phase holdup and total bubble count for the probe oriented at $\theta = 180°$ indicate that there exists a significant number of bubbles that deviate from the main flow direction even for a seemingly unidirectional flow: thus the wording "approximate unidirectional flow" and not "unidirectional flow." In gas-liquid systems, the bubbles always have a very well-defined mean velocity, but considerable variations may exist. When these variations are confined locally, and when globally the mean velocity has a very small variance and is always in one direction, we have unidirectional flow. For such conditions, the probe oriented at $\theta = 180°$ would miss almost all bubbles, as the fiber

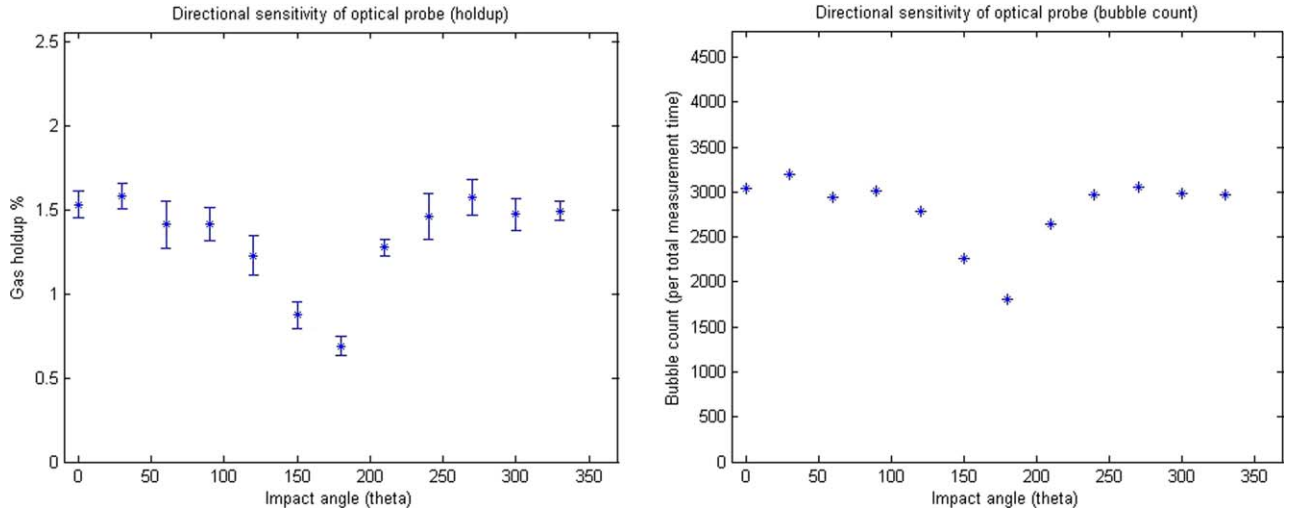

Figure 4. Measured gas holdups and bubble counts at various impact angles for approximate unidirectional flow in the stirred tank.

[Color figure can be viewed in the online issue, which is available at wileyonlinelibrary.com.]

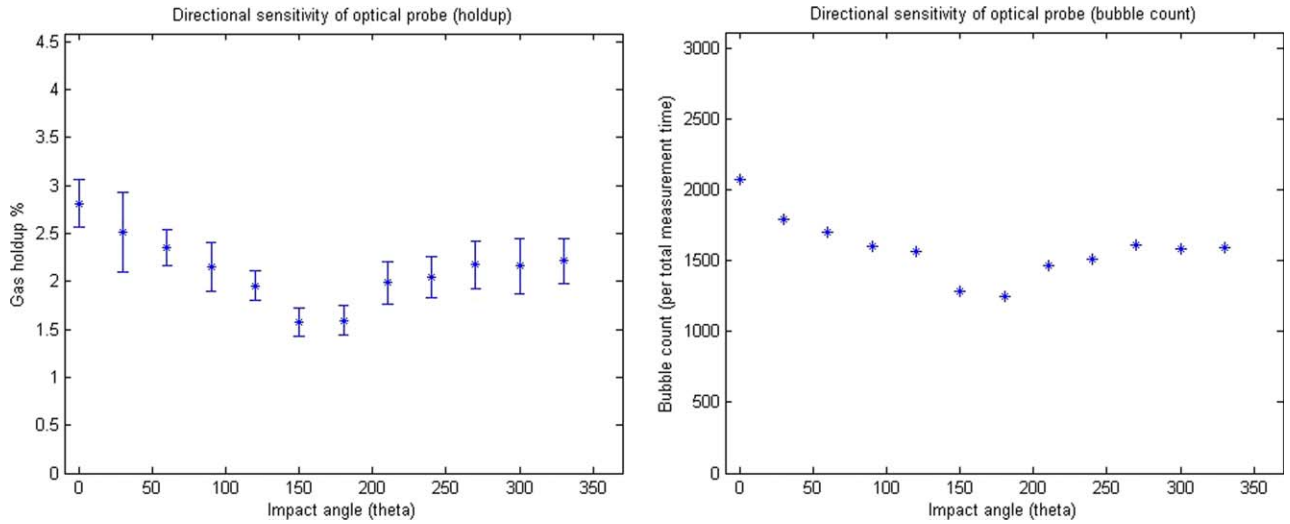

Figure 5. Measured gas holdups and bubble counts at various impact angles for bubbly flow in the stirred tank.

[Color figure can be viewed in the online issue, which is available at wileyonlinelibrary.com.]

and the metal sheathing aligned with the main flow direction would block them from ever reaching and piercing the tip.

Bubbly flows

Figures 5 and 6 show the gas holdups and bubble counts obtained at various impact angles for the two bubbly flow conditions we investigated. The results revealed a similar pattern to that of "unidirectional" flow (a nearly constant gas holdup from impact angles of 0–90°, followed by a decrease for impact angles of 90–180°). Nevertheless, there were two noticeable differences: the magnitudes of the (standard) deviations for gas holdups and the degree of gas phase holdup measured by the probe oriented at $\theta = 180°$ (compared to what was measured at $\theta = 0°$) were higher in the two bubbly flow conditions. For the stirred tank, the gas holdups and bubble counts measured at $\theta = 180°$ were 57 and 60% of those measured at $\theta = 0°$, respectively; for the sparged tank, the ratios were 50 and 75%, respectively. These results suggest the degree of bubble trajectory deviation from the main flow direction to be higher in the bubbly flow conditions.

The Probabilistic Model and Constitutive Equations

As mentioned previously, the magnitude of our optical probes' directional sensitivity, as well as that of other "needle-like" techniques, depends on various attributes such as exact probe tip geometry, curvatures of moving interfaces, evolution of the interface profiles, angle of attack with respect to the tip, and so forth,[24,42] most of which are not available *a priori*. Rather than a detailed theoretical analysis of case-by-case piercing mechanisms that would involve additional assumptions, here we provide a robust model that could be extended to all other "needle-like" probes.

Cone of acceptance angle

Our model is based on one assumption regarding the acceptance angle cone: all bubbles, that is, interfaces, traveling within

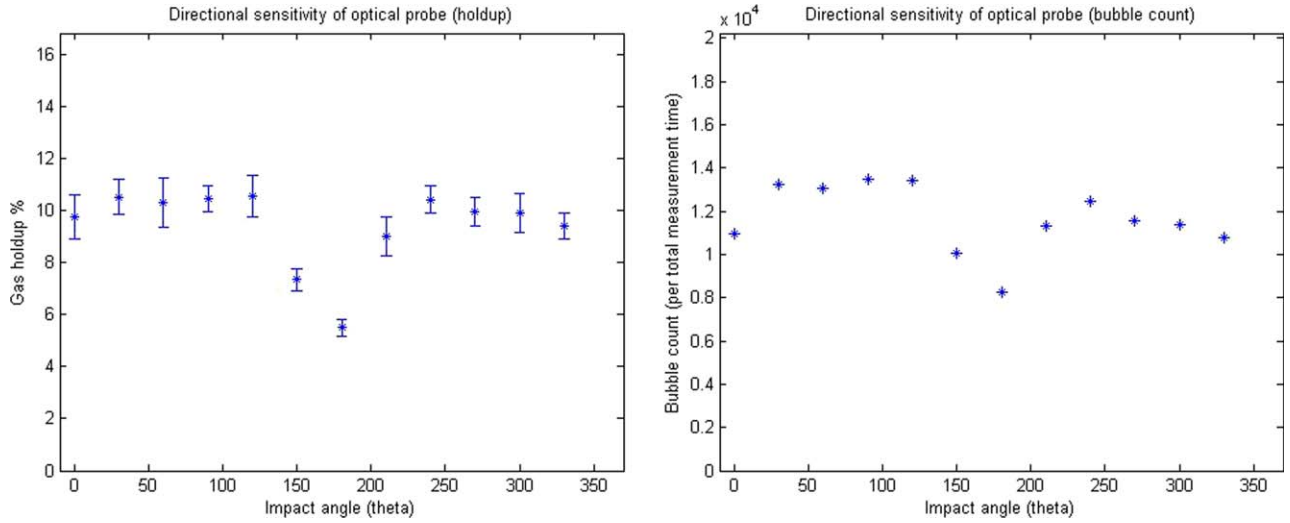

Figure 6. Measured gas holdups and bubble counts at various impact angles for bubbly flow in the sparged tank.

[Color figure can be viewed in the online issue, which is available at wileyonlinelibrary.com.]

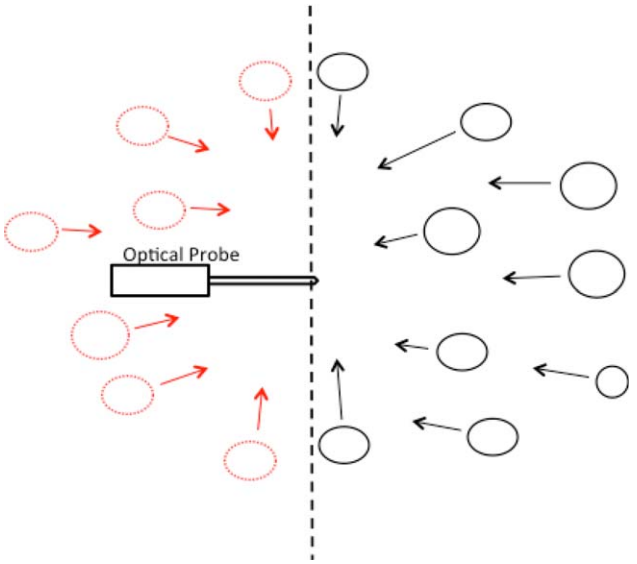

Figure 7. An optical probe ("needle-like" probe) in a gas-liquid system with bubbles moving in various directions.

[Black, solid line circles represent bubbles moving from the right to the left ($\beta \leq 180°$) with respect to the probe tip orientation. Red, dashed line circles represent bubbles moving from the left to the right ($\beta > 180°$) with respect to the probe tip orientation. Our assumption: all bubbles (interfaces) traveling from the right to the left are detected by the probe, whereas only a fraction of those traveling from the left to right are detected.] [Color figure can be viewed in the online issue, which is available at wileyonlinelibrary.com.]

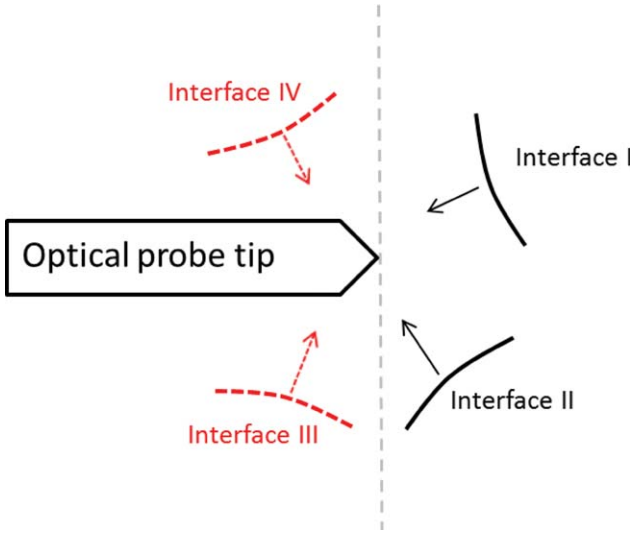

Figure 8. Gas-liquid interfaces (bubbles) approaching the optical probe tip from various directions.

[Black, solid lines represent interfaces moving from the right to the left ($\beta \leq 180°$). Red, dashed lines represent interfaces moving from the left to the right ($\beta > 180°$).] [Color figure can be viewed in the online issue, which is available at wileyonlinelibrary.com.]

the impact angle of 90°, or the acceptance angle (β) of 180°, are successfully captured by the optical probe, while only a fraction of the bubbles traveling at larger angles are captured by the probe. Pictorially, this is represented in Figure 7.

As the probe tips we used are much smaller (105 μm core diameter, detection area $\sim$ 10 μm) than typical bubble sizes observed in standard temperature and pressure gas-liquid systems,[21,29] our assumption can be represented in terms of near-flat bubble interfaces approaching the probe tip, as shown in Figure 8.

According to our assumption, all interfaces travelling within $\beta \leq 180°$ shown in Figure 8 (and therefore, bubbles in Figure 7), that is, interfaces I and II, are successfully detected by the probe, whereas only a fraction of interfaces traveling at $\beta > 180°$, that is, interfaces III and IV, are detected. Two of the most likely mechanisms which cause such behavior include: (1) significant interface-probe interaction which causes certain bubbles traveling at $\beta > 180°$ to move away from the detection area, and (2) smaller bubbles' inability to pierce the probe tip when travelling at $\beta > 180°$. According to this assumption, when not employed in a unidirectional flow region, the optical probe technique always possesses the potential for underestimation of the true local gas phase holdup and bubble count.

Probabilistic description of gas phase dispersions and the model

Treatment of our collected optical measurements in the frequency domain[33] revealed the chaotic nature of bubble occupancy for all positions and conditions we investigated. No noticeable auto or cross correlations were observed, and the likelihood (probability) of a bubble occurrence was statistically independent for measurements collected at different orientations (θ). Figure 9 shows the comparisons of joint probabilities of gas phase occupancy, that is, local gas phase holdup, for the signal taken at $\theta = 0°$ and all other θ's for the bubbly flow condition we investigated in the sparged tank. All joint probabilities were essentially equal to the product of the corresponding individual probabilities, a necessary condition for two

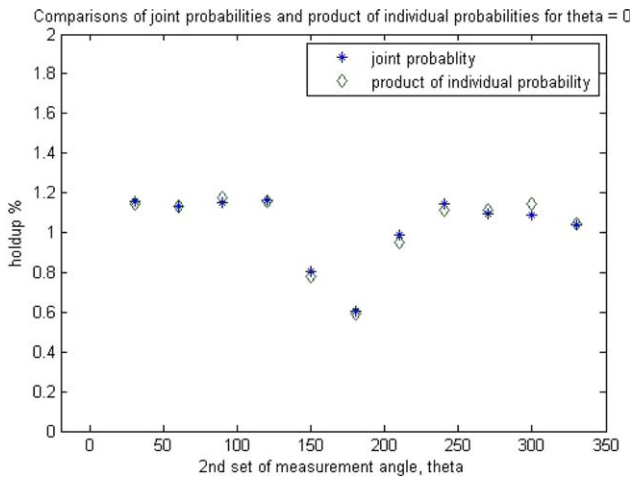

Figure 9. Comparisons between (1) the joint probabilities of gas phase occupancy at $\theta = 0°$ and all other θ's, and (2) the product of the gas phase occupancy at $\theta = 0°$ and all other θ's.

[Results are from bubbly flow investigated in the sparged tank.] [Color figure can be viewed in the online issue, which is available at wileyonlinelibrary.com.]

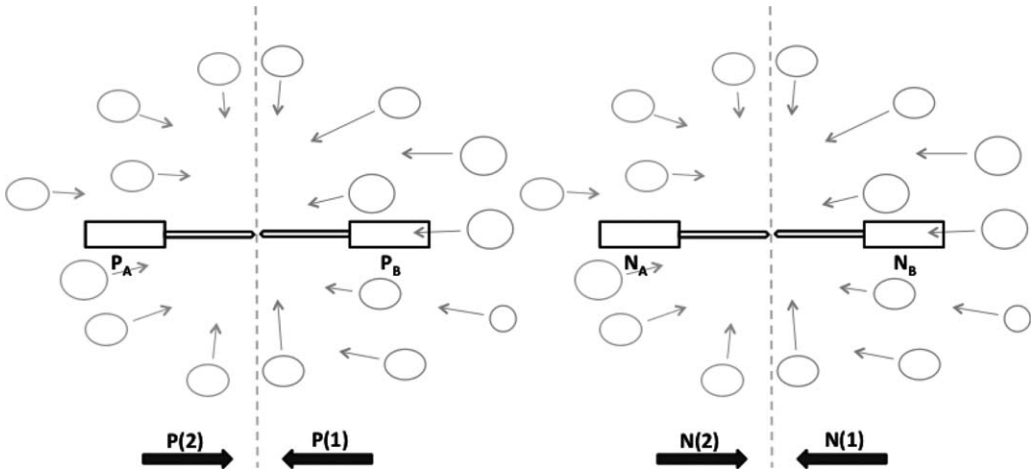

Figure 10. Two sets of measurements at different impact angles.

events being statistically independent. The same relationship was found for two other flow conditions we investigated.

Based on these results and our assumption for the acceptance angle cone, a probabilistic model that separates directional contributions of bubbles from the local gas phase holdup and bubble count was formulated, as shown in Eq. 2 through 5. The model separates contributions to the local gas holdup and bubble count (number of interface boundaries detected) from those traveling in two opposite directions, for example, from left to right and right to left. Figure 10 schematically represents the introduced variables

$$P(A) = P(1) + x_1 \cdot P(2) - x_1 \cdot P(1) \cdot P(2) \tag{2}$$

$$P(B) = P(2) + x_2 \cdot P(1) - x_2 \cdot P(1) \cdot P(2) \tag{3}$$

$$N_A = N(1) + x_1 \cdot N(2) \tag{4}$$

$$N_B = N(2) + x_2 \cdot N(1) \tag{5}$$

In Eq. 2 through 5, P_A and P_B represent the measured probability of gas occupancy for a probe tip oriented in one of two opposite directions; $P(1)$ and $P(2)$ represent the directional probabilities of gas phase holdup due to bubbles traveling toward either probe tip A or B within $\beta \leq 180°$; N_A and N_B represent the number of interface boundaries (bubble counts) detected by either probe tip A or B; $N(1)$ and $N(2)$ represent the number of interfaces traveling toward either probe tip A or B within $\beta \leq 180°$; and x_1 and x_2 represent the fraction of the gas phase holdup and number of interfaces detected by a probe tip for bubbles traveling at angles larger than the cone of acceptance angle, $\beta > 180°$.

The main difference between the two sets of equations (Eqs. 2, 3 and Eqs. 4, 5), which results in two additional terms for the first set ($x_1 \cdot P(1) \cdot P(2)$ for Eq. 2 and $x_2 \cdot P(1) \cdot P(2)$ for Eq. 3), arises from the fact that P_x and N_x measured by the probe have different statistical properties. By the definition of local gas holdup in our algorithms, the measure of gas phase occupancy probability (local gas phase holdup, P_x) is not mutually exclusive, that is, bubbles traveling from two opposite directions ($P(1)$ and $P(2)$) can occupy the same point space simultaneously and contribute to the local gas phase holdup. For bubble counts, this is not the case, as the signal rise resulting from the passing of an interface at the probe tip can only be due to either interface traveling from opposite directions, that is, the total number of interfaces detected by the probe, N_x, is mutually exclusive.

The third set of equations needed to solve for the six introduced parameters, $P(1)$, $P(2)$, $N(1)$, $N(2)$, x_1, and x_2 makes use of the ratio between the two parameters $P(x)$ and $N(x)$, $\frac{P(x)}{N(x)}$, which represents the average amount of time spent by a bubble at a local reactor space (Eq. 6)

$$\frac{P(x)}{N(x)} = \frac{\dfrac{\text{total amount of time spent in gas phase for bubbles traveling in } x-\text{direction}}{\text{total measurement time}}}{\dfrac{\text{total number of bubbles (interfaces) traveling in } x-\text{direction}}{\text{total measurement time}}} = \frac{\text{total amount of time spent in gas phase for bubbles traveling in } x-\text{direction}}{\text{total number of bubbles (interfaces) traveling in } x-\text{direction}} \tag{6}$$

As shown in Figure 11, this ratio is highly direction-dependent as it is a function of local flow properties that include detailed bubble properties such as the velocity, travel direction, and size distribution.

By assuming these measured ratios to be equivalent to the weighted average of the two ratios for two bubble populations traveling in opposite directions, two additional equations can be formulated, as shown in Eqs. 7 and 8

$$\frac{P_A}{N_A} = \frac{\frac{P(1)}{N(1)} + x_1 \frac{P(2)}{N(2)}}{1 + x_1} \tag{7}$$

$$\frac{P_B}{N_B} = \frac{\frac{P(2)}{N(2)} + x_2 \frac{P(1)}{N(1)}}{1 + x_2} \tag{8}$$

Along with Eqs. 2–5, Eqs. 7 and 8 can now be used to solve for the six introduced parameters, from which the true (unbiased) local gas phase holdups and bubble counts can be

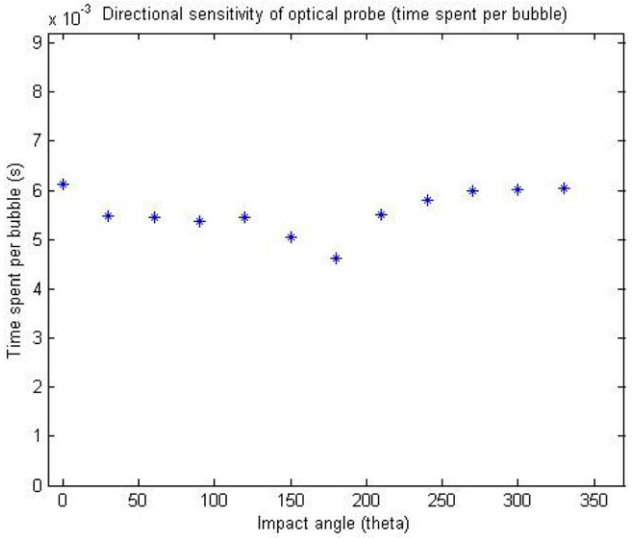

Figure 11. The average amount of time spent per bubble (at the detection area) for the bubbly flow condition in the sparged tank region where our probes were employed.

Similar profiles were observed for the two other operating conditions. [Color figure can be viewed in the online issue, which is available at wileyonlinelibrary.com.]

obtained via Eqs. 9 and 10, and the degree of local gas phase separated into two bubble movement directions

$$\text{Gas holdup}_{\text{true, unbiased}} = P(1)+P(2)-P(1)\cdot P(2) \quad (9)$$

$$\text{Bubble count}_{\text{true, unbiased}} = N(1)+N(2) \quad (10)$$

Results

There are several points within the range of possible solutions where our constitutive equations (Eqs. 2–5, 7, 8) become underdetermined, for example, $x_1, x_2 = 0$, or ill-posed, for example, $N(1) = N(2)$. To avoid these points, ranges of possible solutions listed in Table 1 were included as part of our algorithm. The ranges were determined based on an assumption that the higher the gas holdups and bubble counts measured by the probe (compared to a probe oriented in opposite direction), the more likely the bubbles will travel toward that direction and the higher the fraction of backflow (bubbles traveling at $\beta > 180°$) detected by the probe.

Table 1. Range of Possible Values for the Variables in the Constitutive Model Equations

Variables	Range
$P(1)$	$P_B < P(1) \le P_A$, if $P_A \ge P_B$ $0.1 \cdot P_B < P(1) \le P_B$, if $P_A < P_B$
$P(2)$	$0.1 \cdot P_B < P(2) \le P_B$, if $P_A \ge P_B$ $P_A < P(2) \le P_B$, if $P_A < P_B$
$N(1)$	$N_B < N(1) \le N_A$, if $N_A \ge N_B$ $0.1 \cdot N_B < N(1) \le N_B$, if $N_A < N_B$
$N(2)$	$0.1 \cdot N_B < N(2) \le N_B$, if $N_A \ge N_B$ $N_A < N(2) \le N_B$, if $N_A < N_B$
x_1	$\frac{N_B}{N_A} < x_1 \le 1$, if $N_A \ge N_B$ $0.1 \cdot \frac{N_B}{N_A} < x_1 \le \frac{N_B}{N_A}$, if $N_A < N_B$
x_2	$0.1 \cdot \frac{N_B}{N_A} < x_2 \le \frac{N_B}{N_A}$, if $N_A \ge N_B$ $\frac{N_B}{N_A} < x_2 \le 1$, if $N_A < N_B$

Approximate unidirectional flow

Figures 12–14 show the unbiased local gas phase holdups obtained via Eq. 9, the magnitudes of dispersions that have been separated into contributions from various directions, and the fractions of backflow (bubbles traveling at $\beta > 180°$ of the probe tip) detected by the optical probe, respectively. Because our model requires at least one set of measurements composed of two optical probe measurements taken from tips facing opposite directions, these figures represent results combined from six measurement sets: 0–180°, 30–210°, 60–240°, 90–270°, 120–300°, and 150–330°.

The unbiased local gas phase holdups obtained via Eq. 9 revealed the validity of our constitutive equations and the assumptions for the "unidirectional" flow conditions. For all six sets of measurements, the unbiased local gas phase holdups were found to be equal to each other with a mean value of 1.69% and a standard deviation 0.08%, and directional sensitivity was not observed anymore. Optical probe measurements collected within $\theta = \pm 90°$ were found to be within the measurement error (standard deviation) of the unbiased local gas holdup, suggesting the optical probe technique's usefulness when positioned at "proper" orientations. These results are also in agreement with what has been previously suggested by Mueller[21] and Mueller and Dudukovic[36] (who came to their conclusion after comparing their results to those from noninvasive techniques): (1) one must obtain at least two measurements with tips oriented in opposite orientations and report the larger gas holdup of the two for an accurate measurement of gas phase holdup via optical probe technique, and (2) It is best to have the probe oriented facing the flow direction for regions where the main flow directions are known. Although not shown here, the unbiased bubble counts were also nearly equal to each other for all six measurement sets.

The magnitudes of directional contributions to the local gas phase holdups and bubble counts were found to be near

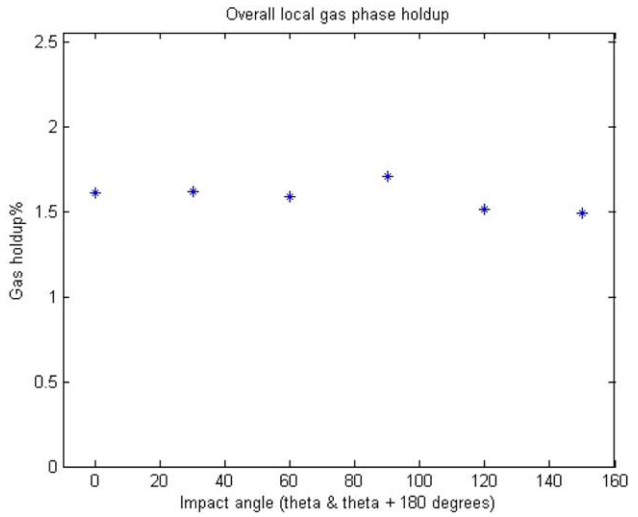

Figure 12. Unbiased local gas phase holdups in a "unidirectional" flow in the stirred tank.

Results from six measurement sets. [Color figure can be viewed in the online issue, which is available at wileyonlinelibrary.com.]

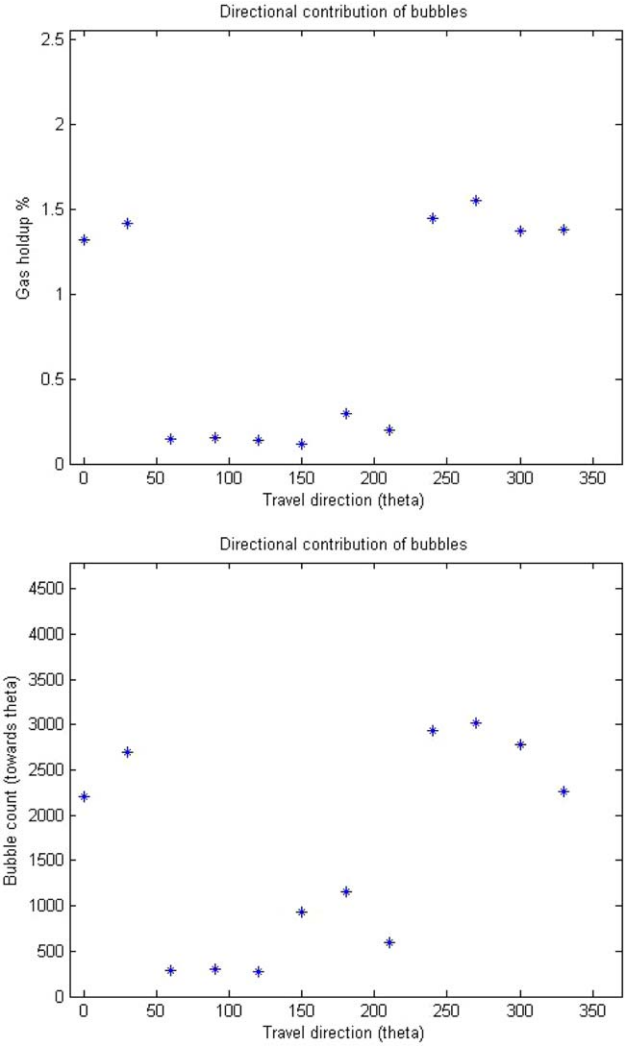

Figure 13. Degree of contribution to the overall local gas phase holdup and bubble count within $\beta \leq 180^\circ$ of θ in a "unidirectional" flow in the stirred tank.

[Color figure can be viewed in the online issue, which is available at wileyonlinelibrary.com.]

their maxima for bubbles traveling within $\beta \leq 180^\circ$ of angles proximate to $\theta = 0^\circ$, that is, $\theta = 0^\circ$, 30°, 240°, 270° 300°, and 330° (Figure 13). The gas phase holdup contributions from bubbles traveling toward the probe tips oriented at $60^\circ \leq \theta \leq 210^\circ$ (within $\beta \leq 180^\circ$ of them) were found to be less than 0.3%, but significant (18.9% of the unbiased local gas phase holdup), suggesting that even for a seemingly unidirectional flow, there exists a small number of bubbles that deviate much from the main flow direction, possibly due to velocity fluctuations caused by eddies of different sizes. These bubbles are most likely traveling toward $\theta \approx 330^\circ$ (-35°), because near constant contributions were observed for $\theta = 0^\circ$, 30°, 240°, 270°, 300°, and 330°. Further investigation and analysis are necessary for a firmer conclusion.

The profile for the degree of backflow detected by the probe (Figure 14) closely resembled the gas holdup and the bubble count profiles shown in the previous section (Figure 4). The fraction of backflow detected was at a near maximum value at angles proximate to $\theta = 0^\circ$, decreased as θ increased up to $\theta = 180^\circ$, reached its minimum value at

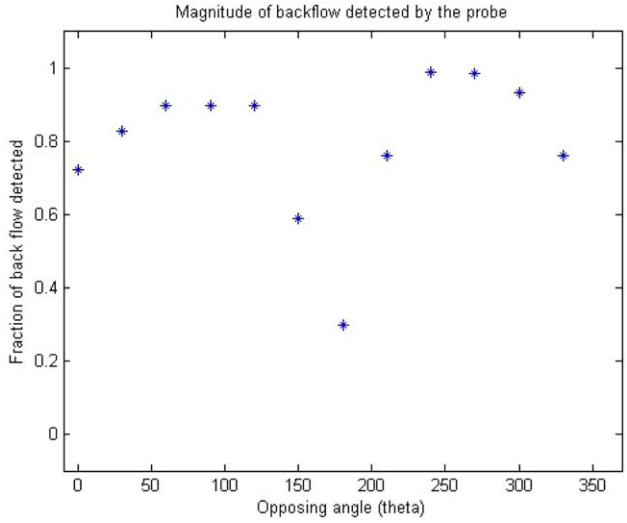

Figure 14. Fraction of backflow detected by the optical probe in a "unidirectional" flow in the stirred tank.

[Color figure can be viewed in the online issue, which is available at wileyonlinelibrary.com.]

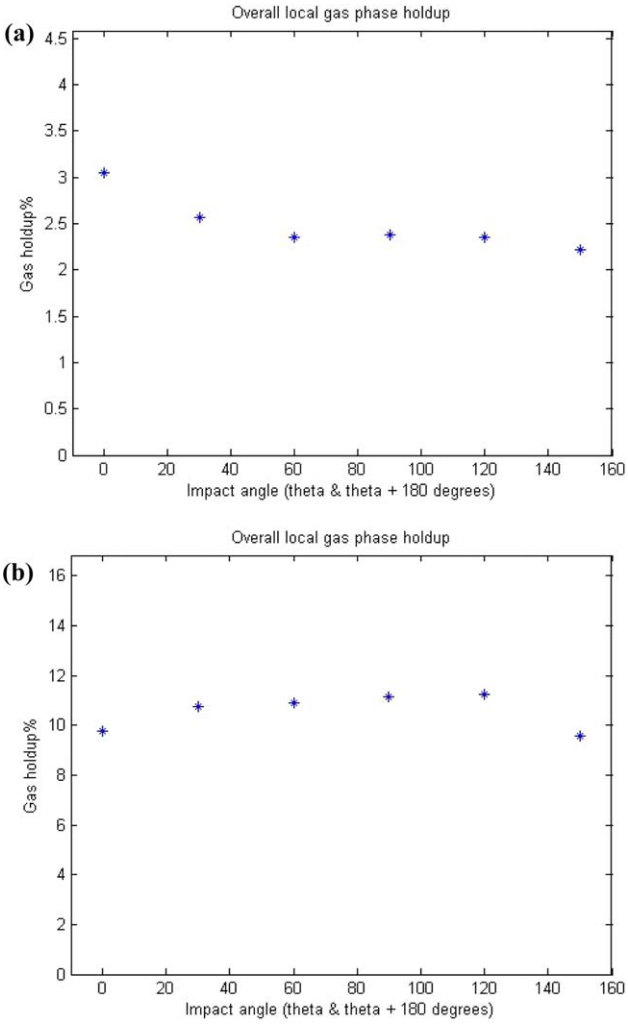

Figure 15. Unbiased local gas phase holdups.

Results from six measurement sets. (a) Bubbly flow condition in the stirred tank; (b) bubbly flow condition in the sparged tank. [Color figure can be viewed in the online issue, which is available at wileyonlinelibrary.com.]

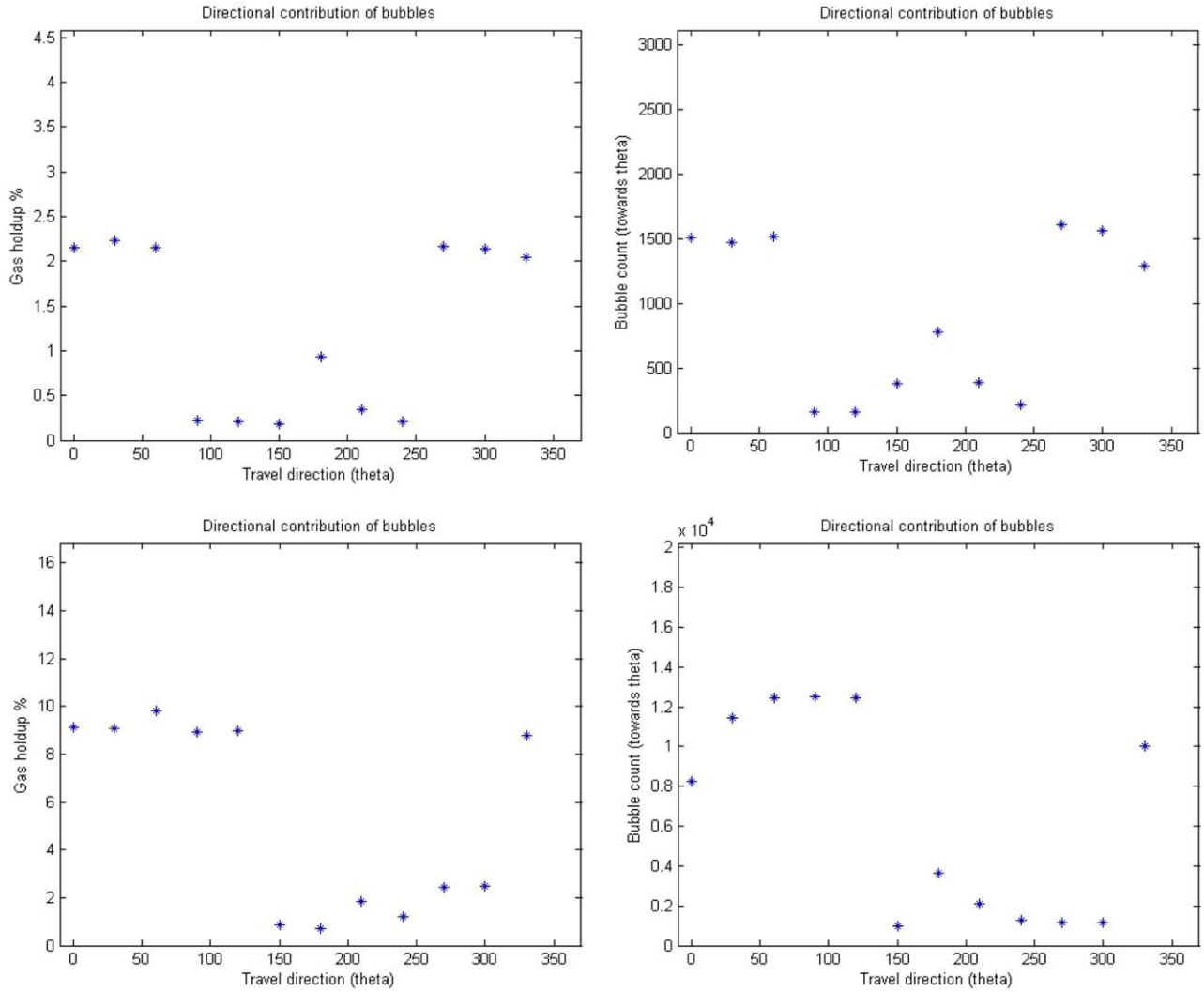

Figure 16. Degree of contributions to the overall gas phase holdup (left) and bubble count (right) within $\beta \leq 180°$ of θ.

Upper figures, bubbly flow condition in the stirred tank; lower figures, bubbly flow condition in the sparged tank. [Color figure can be viewed in the online issue, which is available at wileyonlinelibrary.com.]

$\theta = 180°$, and increased as θ increased up to $\theta = 360°$ (0°). This is consistent with our definition of θ and understanding of the mechanisms responsible for underestimation of gas phase dispersion when the probe is oriented in "improper" directions: the larger the θ (up to 180°), the more likely the probe will interfere with the bubbles traveling along the main flow direction and keep them from ever reaching and being pierced by the probe tip.

Bubbly flows

Figures 15, 16, and 17, respectively, show the unbiased local gas phase holdups, the magnitudes of dispersions that have been separated into contributions from various directions, and the fractions of backflow (bubbles traveling within $\beta > 180°$ of the probe tip) detected by the optical probe for the two bubbly flow conditions we investigated.

As was the case for the "unidirectional" flow, the unbiased local gas holdups revealed the validity of our constitutive equations and the assumptions for the bubbly flow conditions. For the stirred tank, the unbiased local gas holdup was found to be 2.49% with a standard deviation of 0.30%; for the sparged tank, the unbiased local gas holdup was found to be 10.57% with a standard deviation of 0.71% (Figure 15). These values were once again well within the range of what was measured when the optical probe measurements were collected within $\theta = \pm 90°$, suggesting the guideline provided by Mueller and Dudukovic[36] may still be applied in bubbly flow conditions. The unbiased bubble counts were also found to be well within each measurement's range.

The majority of the local gas holdup contribution was found to be due to bubbles traveling along the main flow directions (Figure 16) for the bubbly flow conditions. Contributions from the bubbles traveling against the main flow direction, $\beta \leq 180°$ of $\theta = 180°$, were found to be 30 and 7% of the unbiased local gas phase holdup for the two bubbly flow conditions in the stirred tank and the sparged tank, respectively.

The fraction of the backflow detected by the probe (Figure 17) closely resembled the gas holdup and the bubble count profiles (Figures 5 and 6). The fractions were near their maximum value of 1 at angles proximate to 0°, decreased as θ increased up to 180°, reached its minimum value at $\theta = 180°$, and increased as θ increased back up to $\theta = 360°$ (0°).

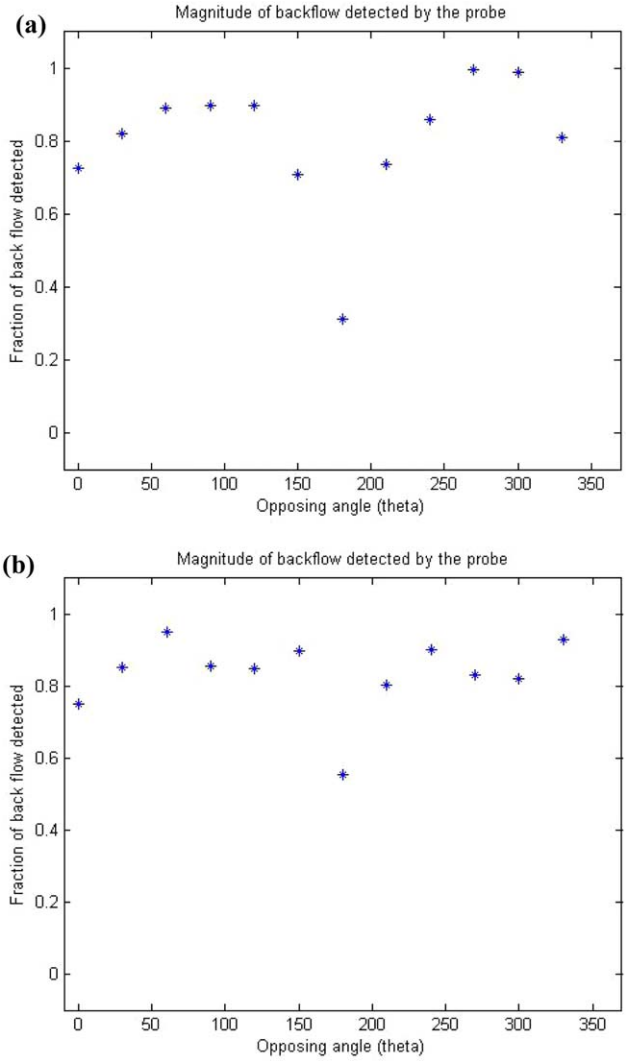

Figure 17. Fraction of backflows detected by the optical probe.

(a) Bubbly flow condition in a stirred tank, (b) bubbly flow condition in the sparged tank. [Color figure can be viewed in the online issue, which is available at wileyonlinelibrary.com.]

Conclusions

A probabilistic model that corrects for the directional sensitivity of the optical probe technique was formulated. The model uses the chaotic nature of the optical probe measurement signals to interpret the measured signals in terms of probability. The model is based on two assumptions. First, all bubbles traveling within the acceptance angle (β) of 180° are successfully captured by the probe. Second, the ratio between the two measured parameter, $\frac{P(x)}{N(x)}$, which represents the average amount of time spent by a bubble at a local reactor space, is a unique property of bubbles traveling in different directions. Application of the model enables separating the contributions of bubbles traveling in different directions to the overall local gas phase holdup and bubble counts. To solve for the six parameters associated with the model, at least two measurements—collected with the probe tips oriented in opposing directions—are needed.

For all three flow conditions we investigated (one "unidirectional" flow and two bubbly flow conditions), the majority of the "unbiased" gas phase holdup was contributed from bubbles traveling within $\beta \leq 180°$ of the main flow direction, that is, $\theta = 0°$. For the "unidirectional" flow condition, approximately 81% of the unbiased local gas phase holdup was due to bubbles traveling within $\beta \leq 180°$ of $\theta = 0°$. For the two bubbly flow conditions, 70 and 93% of the "unbiased" local gas phase holdup was found to be due to bubbles traveling within $\beta \leq 180°$ of the main flow direction for the stirred tank and the sparged tank, respectively. No clear distinction between the two flow conditions in terms of directional contribution was observed.

Significant underestimation, that is, data bias, of the local gas holdup and bubble counts could result from the optical probe measurements if the probe is oriented in the "wrong" directions, that is, $\theta > +90°$ or $\theta < -90°$. The suggestion previously made by Mueller[21] and Mueller and Dudukovic[36] regarding the need for at least two measurements with the probe tip oriented in opposite directions, was found to be effective for all three flow conditions we investigated.

Acknowledgments

The authors would like to thank the Chemical Reaction Engineering Laboratory (CREL) sponsors and the National Science Foundation (Grant: 0933780) for their financial support. Special thanks to Dr. Heinz Schaettler for going over the probabilistic model, Professor James Ballard for reviewing the manuscript, and to Yujian Sun and Zhou Yu of CREL for their thoughtful inputs.

Literature Cited

1. Crowe CT, Schwarzkopf JD, Sommerfeld M, Tsuji Y. *Multiphase Flows with Droplets and Particles*, 2nd ed. Boca Raton, FL: Taylor & Francis, 2011.
2. Balachandar S, Eaton JK. Turbulent dispersed multiphase flow. *Annu Rev Fluid Mech*. 2010;42(1):111–133.
3. Hetsroni G. *Handbook of Multiphase Systems*. USA: Hemisphere Pub. Corp., 1982.
4. Ishii M, Hibiki T. *Thermo-Fluid Dynamics of Two-Phase Flow*. NY: Springer, 2010.
5. Ranade VV. *Computational Flow Modeling for Chemical Reactor Engineering*. San Diego, CA: Academic Press, 2002.
6. Boyer C, Duquenne A-M, Wild G. Measuring techniques in gas–liquid and gas–liquid–solid reactors. *Chem Eng Sci*. 2002;57(16):3185–3215.
7. Chaouki J, Larachi F, Duduković MP. Noninvasive tomographic and velocimetric monitoring of multiphase flows. *Ind Eng Chem Res*. 1997;36(11):4476–4503.
8. Chaouki J, Larachi F, Dudukovic P. *Non-Invasive Monitoring of Multiphase Flows*. Amsterdam, The Netherlands: Elsevier Science, 1997.
9. Zhang Q, Yong Y, Mao Z-S, Yang C, Zhao C. Experimental determination and numerical simulation of mixing time in a gas–liquid stirred tank. *Chem Eng Sci*. 2009;64(12):2926–2933.
10. Khopkar AR, Ranade VV. CFD simulation of gas–liquid stirred vessel: VC, S33, and L33 flow regimes. *AIChE J*. 2006;52(5):1654–1672.
11. Khopkar AR, Rammohan AR, Ranade VV, Dudukovic MP. Gas–liquid flow generated by a Rushton turbine in stirred vessel: CARPT/CT measurements and CFD simulations. *Chem Eng Sci*. 2005;60(8–9):2215–2229.
12. Alves SS, Maia CI, Vasconcelos JMT. Experimental and modelling study of gas dispersion in a double turbine stirred tank. *Chem Eng Sci*. 2002;57(3):487–496.
13. Tryggvason G, Scardovelli R, Zaleski S. Direct Numerical Simulations of Gas–Liquid Multiphase Flows. Cambridge, UK: Cambridge University Press, 2011.
14. Zhang Y, Yang C, Mao Z-S. Large eddy simulation of the gas–liquid flow in a stirred tank. *AIChE J*. 2008;54(8):1963–1974.
15. Derksen J, Van den Akker HEA. Large eddy simulations on the flow driven by a Rushton turbine. *AIChE J*. 1999;45(2):209–221.
16. Guha D, Ramachandran PA, Dudukovic MP, Derksen JJ. Evaluation of large Eddy simulation and Euler-Euler CFD models for solids

flow dynamics in a stirred tank reactor. *AIChE J*. 2008;54(3):766–778.
17. Mudde RF, Van Den Akker HEA. 2D and 3D simulations of an internal airlift loop reactor on the basis of a two-fluid model. *Chem Eng Sci*. 2001;56(21–22):6351–6358.
18. Buffo A, Vanni M, Marchisio DL. Multidimensional population balance model for the simulation of turbulent gas–liquid systems in stirred tank reactors. *Chem Eng Sci*. 2012;70:31–44.
19. Guha D, Dudukovic MP, Ramachandran PA, Mehta S, Alvare J. CFD-based compartmental modeling of single phase stirred-tank reactors. *AIChE J*. 2006;52(5):1836–1846.
20. Hamed ME. *Hydrodynamics, Mixing, and Mass Transfer in Bubble Columns with Internals*. St. Louis, MO: Department of Energy, Environmental, and Chemical Engineering, Washington University, 2012.
21. Mueller SG. *Optical Measurements in Gas-Liquid Stirred Tanks*. St. Louis, MO: Department of Energy, Environmental, and Chemical Engineering, Washington University in St. Louis, 2009.
22. Dudukovic MP. Relevance of multiphase reaction engineering to modern technological challenges. *Ind Eng Chem Res*. 2007;46(25):8674–8686.
23. Bakker A, Van den Akker HEA. A computational model for the gas-liquid flow in stirred reactors. *Chem Eng Res Des*. 1994;72(A4):594–606.
24. Cartellier A. Optical probes for local void fraction measurements: characterization of performance. *Rev Sci Instrum*. 1990;61(2):874–886.
25. Cartellier A. Simultaneous void fraction measurement, bubble velocity, and size estimate using a single optical probe in gas–liquid two-phase flows. *Rev Sci Instrum*. 1992;63(11):5442–5453.
26. Guet S, Fortunati RV, Mudde RF, Ooms G. Bubble velocity and size measurement with a four-point optical fiber probe. *Part Part Syst Charact*. 2003;20(3):219–230.
27. Wang W, Mao Z-S, Yang C. Experimental and numerical investigation on gas holdup and flooding in an aerated stirred tank with Rushton impeller. *Ind Eng Chem Res*. 2006;45(3):1141–1151.
28. Enrique Juliá J, Harteveld WK, Mudde RF, Van den Akker HEA. On the accuracy of the void fraction measurements using optical probes in bubbly flows. *Rev Sci Instrum*. 2005;76(3):035103.
29. Xue J. *Bubble Velocity, Size and Interfacial Area Measurements in Bubble Columns*. St. Louis, MO: Department of Chemical Engineering, Washington University, 2004.
30. Youssef AA. *Fluid Dynamics and Scale-Up of Bubble Columns with Internals*. St. Louis, MO: Department of Energy, Environment, and Chemical Engineering, Washington University, 2010.
31. Wu C. *Heat Transfer and Bubble Dynamics in Slurry Bubble Columns for Fischer-Trpsch Clean Alternative Energy*. St. Louis, MO: Department of Energy, Environmental, and Chemical Engineering, Washington University, 2007.
32. Lee BW, Dudukovic MP. Determination of flow regime and gas holdup in gas–liquid stirred tanks. *Chem Eng Sci*. 2014;109:264–275.
33. Lee BW, Dudukovic MP. Time-series analysis of optical probe measurements in gas–liquid stirred tanks. *Chem Eng Sci*. 2014;116:623–634.
34. Sun Y, Mueller SG, Lee BW, Dudukovic MP. Optical fiber reflectance probe for detection of phase transitions in multiphase systems. *Ind Eng Chem Res*. 2014;53(2):999–1003.
35. Mueller SG, Werber JR, Al-Dahhan MH, Dudukovic MP. Using a fiber-optic probe for the measurement of volumetric expansion of liquids. *Ind Eng Chem Res*. 2007;46(12):4330–4334.
36. Mueller SG, Dudukovic MP. Gas holdup in gas−liquid stirred tanks. *Ind Eng Chem Res*. 2010;49(21):10744–10750.
37. Groen JS. *Scales and Structures in Bubbly Flows. Experimental Analysis of the Flow in Bubble Columns and in Bubbling Fluidized Beds*. Deflt, Netherlands: Delft University of Technology, 2004.
38. Rammohan AR. *Characterization of Single and Multiphase Flows in Stirred Tank Reactors*. St. Louis, MO: Department of Chemical Engineering, Washington University in St. Louis, 2002.
39. Bombač A, Žun I, Filipič B, Žumer M. Gas-filled cavity structures and local void fraction distribution in aerated stirred vessel. *AIChE J*. 1997;43(11):2921–2931.
40. Azzopardi B, Zhao D, Yan Y, Morvan H, Mudde RF, Lo S. *Hydrodynamics of Gas-Liquid Reactors: Normal Operation and Upset Conditions*. Hoboken, NJ: Wiley, 2011.
41. Jiri V, Vecer M, Orvalho S, Sechet P, Ruzicka MC, Cartellier A. Measurement accuracy of a mono-fiber optical probe in a bubbly flow. *Int J Multiphase Flow*. 2010;36(7):533–548.
42. Cartellier A, Achard JL. Local phase detection probes in fluid/fluid two-phase flows. *Rev Sci Instrum*. 1991;62(2):279–303.

Manuscript received Sep. 30, 2014, and revision received Mar. 2, 2015.